EARTH'S CRYOSPHERE
SCIENTIFIC JOURNAL

Earth`s Cryosphere, 2017, vol. XXI, No. 3, pp. 38–44 **http://earthcryosphere.ru/**

RELIABILITY OF BASEMENTS AND STRUCTURES IN CRYOLITHOZONE

DOI: 10.21782/EC2541-9994-2017-3(38-44)

MAXIMUM AND MINIMUM CRITICAL THERMAL LOADS CONSTRAINING THE OPERATION OF THERMOSYPHONS WITH HORIZONTAL EVAPORATOR TUBES (HET)

V.P. Melnikov[1–3], G.V. Anikin[1], A.A. Ishkov[4], S.N. Plotnikov[4], K.A. Spasennikova[4]

[1] *Tyumen State University, 6, Volodarskogo str., Tyumen, 625003, Russia; melnikov@ikz.ru*
[2] *Tyumen Scientific Center, SB RAS, 86, Malygina str., Tyumen, 625026, Russia*
[3] *Tyumen Industrial University, 38, Volodarskogo str., Tyumen, 625000, Russia*
[4] *Earth Cryosphere Institute, SB RAS, P/O box 1230, Tyumen, 625000, Russia; anikin@ikz.ru, a.ishkov1988@yandex.ru, plotnikov59@yandex.ru, kspasennikova@gmail.ru*

The operation of refrigeration systems based on natural convection (two-phase thermosyphons), with horizontal evaporator tubes (HET), is simulated using a previously obtained model. The modeling provides upper and lower constraints on thermal loads at which sustainable operation of the system breaks down. Parameters of the two-phase fluid flow in different system units are calculated at heat fluxes to the evaporator tubes corresponding to the minimum and maximum critical thermal loads. The critical loads are estimated for different system configurations.

Heat and mass transfer, thermosyphon, horizontal evaporator tubes, simulation

INTRODUCTION

Arctic and Subarctic oil and gas fields are becoming progressively more attractive targets for large petroleum companies of Russia. However, building and operation of production and utility structures on permafrost may face problems associated with its degradation and related loss of bearing capacity. The problems can be solved by using seasonal refrigeration systems based on natural convection (two-phase thermosyphons) [*Ershov, 1999; Dolgikh et al., 2015*], including those with horizontal evaporator tubes [*Feklistov et al., 2008*]. Thermosyphons are gaining ever more popularity due to their cost and energy efficiency.

The operation of thermosyphons with horizontal evaporator tubes was accounted for in non-stationary thermal conductivity equations with phase transition obtained previously [*Anikin and Spasennikova, 2012; Dolgikh et al., 2015*].

The present study aims at bracketing the critical thermal loads at which sustainable operation of the cooling system breaks down. As the thermal loads change, the thermodynamic parameters of the coolants change correspondingly. Thus, the coolant parameters can be estimated knowing the maximum and minimum critical thermal loads.

AN HET COOLING SYSTEM

A cooling system based on natural convection (a two-phase thermosyphon), with horizontal evaporator tubes (HET), consists of three units that provide evaporation, condensation, and accelerated circulation of the working fluid (coolant).

The horizontal evaporator tubes are laid in the ground under structures and utilities to cool down and freeze the ground and to keep it frozen. The evaporating unit is a meander-like steel tube with straight and curved segments bent at 90–180°.

The condensing unit rises above the evaporator tubes. The evaporated coolant flows into the condenser by natural convection, condenses to liquid and flows down back to the evaporator by gravity.

The accelerator is a steel tube with its diameter larger than that of the evaporator which ensures separation of the liquid and gas phases of the fluid.

The operation principle of an HET thermosyphon is as follows (Fig. 1): liquid coolant G, which is a sum of two flows G_x and G_y from the condensing and accelerating units, respectively, comes to the evaporator driven by convection and gravity [*Anikin et al., 2011*]. The coolant G exposed to heat flux from the ground boils up at some point of the path length and moves on as a mixture of liquid (G_L) and gaseous

(G_G) phases. The gas-liquid mixture heats up, the liquid evaporates and the gas share increases with the path length.

The operation of an HET system was simulated earlier [*Anikin, 2009; Anikin et al., 2011*]. However, the problem of thermal loads critical for its sustainable operation has never been specially investigated. We are bridging the gap with this study.

OPERATION OF AN HET SYSTEM

The operation of an HET system is considered further using the parameter of a relative evaporator length for convenience:

$$y = \frac{x}{L_{ev}},$$

where L_{ev} is the evaporator length in an HET system; x is the distance from the evaporator input to the current point, ranging from 0 to L_{ev}.

Thus, the relative evaporator length varies from 0 to 1.

According to [*Anikin et al., 2011*], the length of the heated evaporator segment is given by

$$y_{\max} = \frac{(\rho_L g H_c - \Delta p) C_{pL} G}{A_c U},$$

$$A_c = A(T_c), \quad A(T_c) = \frac{dp_{LG}(T_c)}{dT_c},$$

where $y_{\max}$ is the relative path length from the evaporator input to the point where the coolant begins to boil, u.f.; Δp is the pressure gradient required to overcome friction, Pa; ρ_L is the density of the liquid, kg/m^3; g is the gravity acceleration, m/s^2; H_c is the height of the condenser, m; C_{pL} is the specific heat capacity of the liquid at constant pressure, J/kg; G is the fluid flow rate within the heating segment, L/h (hereafter the weight flow rate is converted, for convenience, to L/h of liquid fluid as $[G{\cdot}1000{\cdot}3600]/\rho_L$); $dp_{LG}(T_c)$ is the pressure of saturated vapor as a function of condenser temperature; U is the total heat output to the evaporator, W.

According to numerous calculations [*Anikin, 2009; Anikin et al., 2011; Anikin and Spasennikova, 2012*], Δp is much less than $\rho_L g H_c$ and can be neglected without compromising accuracy. Then,

$$y_{\max} = \frac{\rho_L g H_c C_{pL} G}{A_c U}.$$

Thus, an HET system includes two essential segments where the coolant heats up ($0 < y \leqslant y_{\max}$) and boils ($y_{\max} < y \leqslant 1$).

The maximum and minimum critical thermal loads on the evaporator (heat flux from the ground), at which sustainable system operation of the thermosyphon system fails, are estimated assuming uniform heating of the evaporator q = const). The system can operate at

$$q_{\rm cr}^{\min} < q < q_{\rm cr}^{\max}.$$

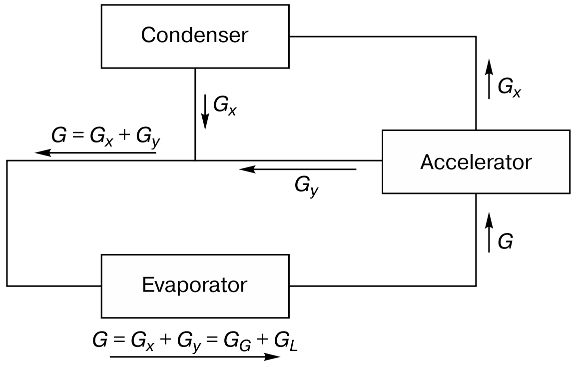

Fig. 1. A two-phase thermosyphon with horizontal evaporator tubes (HET). See text for explanation.

The upper thermal loads $q_{\rm cr}^{\max}$ were discussed in many publications (e.g., [*Butterworth and Hewitt, 1977*]). As applied to an HET system, a heat flux to the evaporator tube exceeding the maximum critical thermal load $\left(q \geq q_{\rm cr}^{\max}\right)$ provides rapid (almost instant) boiling of the coolant, while the heating segment is extremely short: $y_{\max} << 1$. Then all fluid experiences a phase change (liquid converts to gas) at an evaporator segment of a small length $y < 1$, and only gas arrives at the output. The system operation obviously fails.

If the heat flux to the evaporator is below the minimum critical load $\left(q \leq q_{\rm cr}^{\min}\right)$, $0.5 < y_{\max} < 1$, the heating segment is long, and the operation of the cooling system becomes inefficient, though it may continue. Indeed, if the heating segment becomes too long or occupies the entire evaporator path ($y_{\max} = 1$), the system cannot operate. However, a real system fails at any $y_{\max} < 1$.

SIMULATION OF AN HET SYSTEM

The operation of an HET cooling system was simulated using a forward model from [*Anikin, 2009; Anikin et al., 2011*].

The main equation of such a system (its derivation is omitted) is

$$\varphi_G(1)(\rho_L - \rho_G) g H_c = \frac{\xi(\mathrm{Re}_L, \bar{\Delta}) L_y}{D} \frac{G_y^2}{2S_t^2 \rho_L} +$$

$$+ \frac{\xi(\mathrm{Re}_L, \bar{\Delta})(L_{\rm un} + y_{\max} L_{ev})}{D} \frac{G^2}{2S_t^2 \rho_L} +$$

$$+ \int_{y_{\max}}^{1} \Phi_L^2(y') \xi(\mathrm{Re}_L(y'), \bar{\Delta}) \frac{G_L(y')^2}{2DS_t^2 \rho_L} \frac{U}{q(y')} dy' +$$

$$+ \Phi_L^2(1) \frac{\xi(\mathrm{Re}_L, \bar{\Delta})}{D} \frac{(G_L(1))^2 L_z}{2S_t^2 \rho_L} + \Delta p U,$$

$$\Delta pU = \rho_L \left(v_L(1)\right)^2 \varphi_L(1) + \rho_L \left(v_G(1)\right)^2 \varphi_G(1) - \rho_L \left(v_L(0)\right)^2,$$

where $\varphi_G(1)$ is the true volumetric gas content at the evaporator output, u.f.; $\varphi_L(1)$ is the true volumetric liquid content at the evaporator output, u.f.; $\Phi_L^2(1)$ is the dimensionless empirical correction coefficient; $\xi\left(\mathrm{Re}_x, \bar{\Delta}\right)$ is the friction drag depending on Reynolds number and relative roughness of the tube surface; D is the tube diameter, m; S_t^2 is the tube cross section area, m^2; $G_L(y)$ is the flow rate of liquid, L/h; q is the heat flux per tube unit length, W/m; L_y is the path length between the accelerator output and the confluence of the G_x and G_y flows (node), m; L_z is the path length from the evaporator output to the accelerator input, m; L_{un} is the path length from the node to the evaporator input, m; $v_L(0)$ and $v_L(1)$ are the true liquid velocities at the evaporator input and output, m/s; $v_G(1)$ is the true gas velocity at the evaporator output, m/s.

The first term of the equation refers to the pressure gradient in the liquid between the accelerator output and the evaporator input; the second and third terms refer to the total pressure gradient required to overcome friction within the tube segment filled with liquid only; the fourth term corresponds to pressure drop to zero at the account of friction within the phase change segment; the fifth term is the pressure gradient required to overcome friction in the tubes; and the sixth term is the pressure gradient due to acceleration of the gas-liquid mixture. According to [*Idelchik, 1992*], the friction drag is

$$\xi\left(\mathrm{Re}, \bar{\Delta}\right) = \xi_1(\mathrm{Re})\left(1 - p_1(\mathrm{Re})\right) +$$

$$+\xi_2(\mathrm{Re}) p_1\left(\mathrm{Re}\right)\left(1 - p_2\left(\mathrm{Re}, \bar{\Delta}\right)\right) + \xi_3\left(\bar{\Delta}\right) p_1(\mathrm{Re}) p_2\left(\mathrm{Re}, \bar{\Delta}\right),$$

where

$$\xi_1(\mathrm{Re}) = \frac{64}{\mathrm{Re}};\ \ \xi_2(\mathrm{Re}) = \frac{0.3164}{\mathrm{Re}^{0.25}};$$

$$\xi_3\left(\bar{\Delta}\right) = \left(1.8\ \log\frac{8.3}{\bar{\Delta}}\right)^{-2};$$

$$\bar{\Delta} = \frac{\delta h}{D};\ \ \mathrm{Re} = \frac{GD}{S_t \mu};\ \ p_1(\mathrm{Re}) = 0.5\left(1 + \mathrm{erf}\left(\frac{\mathrm{Re} - 2850}{600\sqrt{2}}\right)\right);$$

$$p_2\left(\mathrm{Re}, \bar{\Delta}\right) = \mathrm{erf}\left(\frac{\mathrm{Re}\bar{\Delta}}{275\sqrt{2}}\right).$$

δh is the absolute roughness of the tube surface, m; μ is the dynamic viscosity of a single-phase flow, Pa·s.

Table 1. **Constant C at different flow regimes of liquid and gas coolant phases in the HET system**

Liquid	Gas	C constant
Turbulent	Turbulent	20
Laminar	Turbulent	12
Turbulent	Laminar	10
Laminar	Laminar	5

The coefficient Φ_L^2 necessary for conversion from single-phase to two-phase flow is found as

$$\Phi_L^2 = 1 + \frac{C}{X} + \frac{1}{X^2};$$

$$X = \left(\frac{\xi\left(\mathrm{Re}_L, \bar{\Delta}\right)}{D}\frac{G_L^2}{2S_t^2 \rho_L}\right)^{1/2}\left(\frac{\xi\left(\mathrm{Re}_G, \bar{\Delta}\right)}{D}\frac{G_G^2}{2S_t^2 \rho_G}\right)^{-1/2},$$

where X is the Lockhart-Martinelli parameter and C is constant (Table 1).

For $\varphi_G(y)$ and $\varphi_L(y)$, the following equations are valid [*Crowe, 2006*]:

$$\varphi_L(y) = \frac{1}{\left(\Phi_L^2(y)\right)^{1/3}},\ \ \varphi_G(y) = 1 - \varphi_L(y).$$

The simulation for ammonia used as coolant (see Table 2 for its thermal properties) led to the following results. The maximum and minimum critical thermal loads were estimated using user-specified heat flux as input condition: q was assumed to increase uniformly from 0 to 150, at a stepsize of 0.01. Then a simulation cycle with respect to q was started, and multiple solutions could be found by fitting. Note that not every q value can lead to the solution of the system, and the obtained solutions may be fewer than the heat flux values. The first and last solutions corresponded, respectively, to the minimum $\left(q_{\mathrm{cr}}^{\mathrm{min}}\right)$ and maximum $\left(q_{\mathrm{cr}}^{\mathrm{max}}\right)$ critical thermal loads. At high thermal loads q, a solution always exists, so we choose the value q that corresponds to complete evaporation (only gas comes to the evaporator output). This is the maximum critical thermal load $q_{\mathrm{cr}}^{\mathrm{max}}$.

The minimum critical thermal load values $q_{\mathrm{cr}}^{\mathrm{min}}$ are given in Table 3 for different heights of the condenser above the evaporator H_c; evaporator lengths L_{ev}; and the fluid temperatures in the condenser T_c in Celsius degrees ($t_c = T_c - 273.15$).

The parameters of the HET system at the minimum critical load are given in Tables 4 and 5: t_{av} is the average temperature in the evaporator, °C; t_{max} is the maximum temperature in the evaporator, °C; t_{out} is the temperature at the evaporator output, °C; $\chi_G(1)$ is the gas content at the evaporator output, u.f.; U is the total heat of the HET system, W; $f = G_L(1)/G_G(1)$; R_{in} is the true inner thermal resistance of the HET system, °C/W; R_{in}^0 is the approximate analytical thermal resistance, °C/W.

The internal thermal resistance values R_{in}^0 and R_{in} are

$$R_{\mathrm{in}}^0 = \frac{0.5\rho_L g H_c}{UA_c};\ \ R_{\mathrm{in}} = \frac{t_{ev} - t_c}{U},$$

where t_{ev}, t_c are the evaporator and condenser temperatures, respectively, °C.

Table 2. **Thermal properties of ammonia**

t, °C	$\eta_G \cdot 10^{-5}$	$\eta_L \cdot 10^{-3}$	Cp_L, J/kg	$r_{LG} \cdot 10^6$, J/m^3	ρ_L	ρ_G
	m^2/s				kg/m^3	
–60	0.710	0.380	4370	1.441	713.70	0.214
–40	0.790	0.280	4440	1.389	690.16	0.647
–20	0.890	0.230	4510	1.329	664.93	1.609
0	0.950	0.190	4600	1.263	638.48	3.464
20	1.030	0.154	4720	1.188	610.29	6.701
40	1.120	0.126	4900	1.101	579.43	12.038

Note. t = temperature; η_G = kinematic viscosity of gas fluid phase; η_L = kinematic viscosity of liquid fluid phase; Cp_L = heat capacity of liquid; r_{LG} = latent phase change heat; ρ_L = density of liquid; ρ_G = density of gas.

Table 3. **Minimum critical thermal loads (W/m) for different parameters of an HET thermosyphon system**

H_c, m	L_{ev}, m	t_c, °C		
		–40	–20	0
2.5	200	8.92	4.00	2.92
2.5	400	3.25	1.15	0.76
5.0	200	20.80	11.88	5.77
5.0	400	7.45	4.38	2.02

Table 4. **Parameters of an HET thermosyphon system at H_c = 2.5 m, L_{ev} = 200 and 400 m and minimum critical thermal load**

Estimated parameters	System geometry					
	H_c = 2.5 m, L_{ev} = 200 m			H_c = 2.5 m, L_{ev} = 400 m		
	Condenser temperature t_c, °C					
	–40	–20	0	–40	–20	0
q_{cr}^{min}, W/m	8.92	4.00	2.92	3.25	1.15	0.76
t_{av}, °C	–37.72	–19.05	0.61	–37.71	–19.04	0.62
t_{max}, °C	–36.23	–18.46	0.86	–36.22	–18.43	0.88
t_{out}, °C	–38.34	–18.85	0.68	–38.36	–18.58	0.77
$G_L(1)$, L/h	262.24	410.04	379.63	183.26	257.31	221.87
$G_L(0)$, L/h	268.95	413.30	382.24	188.15	259.19	223.23
$G_G(1)$, L/h	6.70	3.26	2.61	4.88	1.87	1.36
$\chi_G(1)$, u.f.	0.025	0.008	0.007	0.03	0.01	0.01
$\varphi_G(1)$, u.f.	0.62	0.40	0.31	0.63	0.27	0.21
Δp, 10^4 Pa	1.05	0.66	0.48	1.06	0.43	0.32
$\Sigma\Phi_L$, 10^3 Pa	8.28	3.01	2.75	8.94	1.56	1.83
ΔpX, 10^3 Pa	1.12	2.94	1.70	1.06	2.63	1.34
ΔpL, 10^3 Pa	1.09	0.59	0.31	0.59	0.13	0.08
ΔpU, Pa	35.28	22.15	11.46	17.99	5.18	2.44
$v_G(1)$, m/s	6.01	1.75	0.82	4.35	1.52	0.63
$v_L(1)$, m/s	0.36	0.36	0.29	0.26	0.18	0.15
$v_L(0)$, m/s	0.14	0.22	0.20	0.10	0.14	0.12
U, W	1784	800	584	1300	460	304
f	39.13	125.80	145.58	37.53	137.29	163.44
y_{max}, u.f.	0.53	0.68	0.46	0.51	0.76	0.53
R_{in}^0, 10^{-4} °C/W	1.23	1.21	0.83	1.69	2.10	1.60
R_{in}, 10^{-4} °C/W	1.28	1.19	1.05	1.76	2.08	2.04
R_{in}^0/R_{in}	0.96	1.01	0.80	0.96	1.01	0.79

Table 5. **Parameters of an HET thermosyphon system at H_c = 5 m, L_{ev} = 200 and 400 m and minimum critical thermal load**

Estimated parameters	System geometry					
	H_c = 5 m, L_{ev} = 200 m			H_c = 5 m, L_{ev} = 400 m		
	Condenser temperature t_c, °C					
	–40	–20	0	–40	–20	0
q_{cr}^{min}, W/m	20.80	11.88	5.77	7.45	4.38	2.02
t_{av}, °C	–35.75	–18.03	1.01	–35.72	–18.00	0.98
t_{max}, °C	–32.79	–16.79	1.59	–32.77	–16.76	1.56
t_{out}, °C	–37.43	–18.18	1.25	–37.45	–18.21	1.26
$G_L(1)$, L/h	270.40	489.58	569.41	185.73	342.04	419.50
$G_L(0)$, L/h	286.03	499.26	574.56	196.92	349.17	423.11
$G_G(1)$, L/h	15.63	9.68	5.15	11.19	7.14	3.61
$\chi_G(1)$, u.f.	0.055	0.019	0.009	0.06	0.02	0.01
$\varphi_G(1)$, u.f.	0.71	0.53	0.36	0.71	0.54	0.35
Δp, 10^4 Pa	2.39	1.72	1.12	2.40	1.75	1.10
$\Sigma\Phi_L$, 10^3 Pa	20.14	11.70	5.23	21.60	13.04	4.92
ΔpX, 10^3 Pa	1.21	3.79	5.12	1.10	3.51	5.60
ΔpL, 10^3 Pa	2.48	1.69	0.84	1.29	0.91	0.46
ΔpU, Pa	101.37	60.68	33.25	50.75	30.99	17.45
$v_G(1)$, m/s	12.33	3.95	1.38	8.79	2.87	0.99
$v_L(1)$, m/s	0.48	0.54	0.47	0.34	0.39	0.34
$v_L(0)$, m/s	0.15	0.26	0.30	0.10	0.18	0.22
U, W	4160	2376	1154	2980	1752	808
f	17.30	50.57	110.50	16.59	47.92	116.27
y_{max}, u.f.	0.50	0.60	0.66	0.48	0.57	0.68
R_{in}^0, 10^{-4} °C/W	1.06	0.81	0.84	1.47	1.10	1.21
R_{in}, 10^{-4} °C/W	1.02	0.83	0.87	1.44	1.14	1.21
R_{in}^0/R_{in}	1.03	0.98	0.97	1.03	0.96	0.99

Table 6. **Maximum critical thermal loads (W/m) for different parameters of an HET thermosyphon system**

H_c, m	L_{ev}, m	t_c, °C		
		–40	–20	0
2.5	200	49.11	71.50	91.22
2.5	400	16.96	24.58	32.75
5.0	200	72.77	103.70	128.49
5.0	400	25.35	36.74	46.48

The HET system arrives at a boiling crisis at the maximum critical thermal load q_{cr}^{max}, with only gas at the evaporator output, therefore, $f = 0$, $\chi_G(1) = 1$, $\varphi_G(1) = 1$.

Table 6 lists q_{cr}^{max} estimates; tables 7 and 8 give the parameters of a two-phase flow at $q = q_{cr}^{max}$.

DISCUSSION

The operation of the HET system was investigated for extended ranges of temperature conditions (–40, –20 and 0 °C) and design geometric parameters (H_c = 2.5, 5.0 m, L_{ev} = 200, 400 m).

The simulation of an HET system subject to highest and lowest critical thermal loads shows that average, maximum, and output temperatures do not differ much. However, the temperature at the evaporator output is almost equal to that of the condenser at the heat flux corresponding to the maximum thermal load. It means that the system operates at its stability limit: all input liquid converts to gas at the output. Thus, all fluid available in the system flows toward the condenser as a gas phase where it converts back to liquid while heat is released into the air. Rapid heat exchange of the gaseous fluid with the inner surface of the condenser is more than three times

Table 7. **Parameters of an HET thermosyphon system at H_c = 2.5 m, L_{ev} = 200 and 400 m and maximum critical thermal load**

Estimated parameters	System geometry					
	H_c = 2.5 m, L_{ev} = 200 m			H_c = 2.5 m, L_{ev} = 400 m		
	Condenser temperature t_c, °C					
	−40	−20	0	−40	−20	0
q_{cr}^{min}, W/m	49.11	71.50	91.22	16.96	24.58	32.75
t_{av}, °C	−37.92	−19.04	0.50	−37.92	−19.03	0.50
t_{max}, °C	−35.99	−18.14	0.96	−35.99	−18.14	0.96
t_{out}, °C	−39.86	−19.93	0.03	−39.84	−19.92	0.04
$G_L(0)$, L/h	37.64	59.12	82.24	25.99	40.82	59.17
$G_G(1)$, L/h	36.90	58.26	81.47	25.48	40.06	58.50
Δp, 10^4 Pa	1.64	1.58	1.51	1.63	1.56	1.50
$\Sigma\Phi_L$, 10^4 Pa	1.50	1.45	1.40	1.56	1.50	1.45
ΔpX, Pa	4.15	6.37	13.16	3.37	3.72	6.68
ΔpL, 10^3 Pa	1.09	1.00	0.82	543.66	0.50	0.44
ΔpU, Pa	283.03	263.08	219.38	0.14	125.24	113.75
$v_G(1)$, m/s	21.26	13.01	8.10	14.74	9.01	5.85
$v_L(0)$, m/s	0.020	0.031	0.043	0.014	0.021	0.031
U, W	9822	14 300	18 244	6784	9832	13 100
y_{max}, u.f.	0.014	0.007	0.004	0.014	0.007	0.004
R_{in}^0, 10^{-4} °C/W	2.24	0.67	0.27	3.24	0.98	0.37
R_{in}, 10^{-4} °C/W	2.11	0.67	0.27	3.07	0.99	0.38
R_{in}^0/R_{in}	1.06	1.00	0.98	1.05	0.99	0.97

Table 8. **Parameters of an HET thermosyphon system at H_c = 5 m, L_{ev} = 200 and 400 m and maximum critical thermal load**

Estimated parameters	System geometry					
	H_c= 5 m, L_{ev} = 200 m			H_c = 5 m, L_{ev}= 400 m		
	Condenser temperature t_c, °C					
	−40	−20	0	−40	−20	0
q_{cr}^{min}, W/m	72.77	103.70	128.49	25.35	36.74	46.48
t_{av}, °C	−36.16	−18.14	0.98	−36.14	−18.13	0.98
t_{max}, °C	−32.56	−16.39	1.89	−32.56	−16.39	1.89
t_{out}, °C	−39.75	−19.89	0.06	−39.72	−19.87	0.07
$G_L(0)$, L/h	55.78	84.92	115.69	38.86	60.69	83.82
$G_G(1)$, L/h	54.67	83.99	114.75	38.11	59.88	83.02
Δp, 10^4 Pa	3.29	3.17	3.03	3.28	3.15	3.02
$\Sigma\Phi_L$, 10^4 Pa	2.99	2.91	2.83	3.13	3.02	2.91
ΔpX, Pa	8.82	19.45	30.12	7.28	9.85	18.24
ΔpL, 10^3 Pa	2.32	2.00	1.59	1.16	1.05	854.18
ΔpU, Pa	619.23	543.41	433.29	301.76	277.53	227.81
$v_G(1)$, m/s	31.40	18.64	11.36	21.95	13.36	8.26
$v_L(0)$, m/s	0.029	0.044	0.061	0.020	0.032	0.044
U, W	14 554	20 614	25 698	10 144	14 696	18 592
y_{max}, u.f.	0.029	0.013	0.007	0.029	0.013	0.007
R_{in}^0, 10^{-4} °C/W	3.02	0.94	0.38	4.33	1.31	0.52
R_{in}, 10^{-4} °C/W	2.64	0.90	0.38	3.80	1.27	0.53
R_{in}^0/R_{in}	1.14	1.04	1.00	1.14	1.03	0.99

faster than that corresponding to the minimum thermal load.

The total heat capacity of an HET system is markedly different (by a factor of 3 to 43) at lower and upper thermal load limits, other conditions being equal.

The maximum and minimum critical thermal loads also depend on the condenser height (H_c) and the evaporator length (L_{ev}). Namely, at fixed H_c and variable L_{ev}, both upper and lower critical thermal loads differ by a factor of 1.48 on average, i.e., both q_{cr}^{min} and q_{cr}^{max} are 1.48 times lower at L_{ev} = 400 m than at L_{ev} = 200 m. However, the ratios are different at fixed L_{ev} and variable H_c: 2.67 for the minimum critical thermal loads and 1.46 for the upper limit.

The knowledge of the upper and lower constraints on critical thermal loads of an HET thermosyphon are indispensable for estimating its working efficiency in different conditions. For instance, the distance between tubes (spacing) is not subject to any special norms in the common practice. Meanwhile, such a parameter as the optimal tube spacing (Δz_{opt}) corresponds to an optimal heat flux (q_{opt}) per tube unit length. In fact, Δz_{opt} is the spacing of evaporator tubes at which (i) the ground around the tubes stays completely frozen; and (ii) the tubes experience minor or no temperature (heat flux) influence of the neighbor tubes. At a tube spacing twice shorter than the optimal value ($\Delta z_{opt}/2$), the heat flux to the evaporator tubes is twice lower correspondingly, and the system fails at $q = q_{opt}/2 < q_{cr}^{min}$. On the other hand, at a too large tube spacing (e.g., $2\Delta z_{opt}$), the ground becomes only partly frozen and loses bearing capacity.

CONCLUSIONS

1. The minimum critical thermal load corresponding to the lowest heat flux at which sustainable operation of an HET thermosyphon fails has been introduced for the first time.

2. Simulation using the previously obtained model of an HET cooling system has provided first constraints on the critical thermal loads at different system geometries (the condenser height, H_c, and the evaporator length, L_{ev}). At H_c = 2.5 m and L_{ev} = 200 m and the condenser temperatures −40, −20 and 0 °C, the minimum and maximum critical thermal loads are, respectively, 8.92, 4.00, 2.92 W/m and 49.11, 71.50, 91.22 W/m. At H_c = 5 m and L_{ev} = 200 m, the respective values are 20.80, 11.88, 5.77 W/m and 72.77, 103.70, 128.49 W/m. At H_c = 2.5 m and L_{ev} = 400 m, they are 3.25, 1.15, 0.76 W/m and 16.96, 24.58, 32.75 W/m. The lower and upper limits for a system design with H_c = 5 m and L_{ev} = 400 m are, respectively, 7.45, 4.38, 2.02 W/m and 25.35, 36.74, 46.48 W/m. The system operation fails when the thermal loads reach the critical values.

3. The parameters of two-phase fluid flow in the HET system have been estimated for the minimum and maximum critical thermal loads.

4. The reported results can be used to predict the thermal state of ground under various structures and utilities which is frozen by two-phase thermosyphons with horizontal evaporator tubes, and to choose the optimal design and installation strategies in refrigeration practice.

References

Anikin, G.V., 2009. Simulating the Operation of Cooling Systems with Horizontal Tubes. IKZ, Moscow, Deposited at VINITI 30.10.2009, No. 674-V2009. (in Russian)

Anikin, G.V., Spasennikova, K.A., 2012. Computer modelling of the ground cooling system under the oil-tank. Kriosfera Zemli XVI (2), 60–64.

Anikin, G.V., Plotnikov, S.N., Spasennikova, K.A., 2011. Computer simulation of heat-mass exchange in the systems of horizontal ground cooling. Kriosfera Zemli XV (1), 33–39.

Butterworth, D., Hewitt, G.F. (Eds.), 1977. Two-phase flow and heat transfer. Oxford University Press (Harwell Series), 514 pp.

Crowe, C.T., 2006. Multiphase Flow Handbook. Boca Raton London New York, Taylor&Francis, 1156 pp.

Dolgikh, G.M., Anikin, G.V., Rilo, I.P., Spasennikova, K.A., 2015. Statistical modelling of “GET” system installed at the base of oil reservoir. Earth’s Cryosphere XIX (1), 70–77.

Ershov, E.D. (Ed.), 1999. Fundamentals of Geocryology. Part 5. Engineering Geocryology. Moscow University Press, Moscow, 526 pp. (in Russian)

Feklistov, V.N., Dolgikh, G.M., Okunev, S.N., Pazderin, D.S., 2008. Investigation into HET thermosyphons for soil stabilization, in: Resources of Polar and Highland Areas. State and Prospects of Geocryology. Proc. Intern. Conf. Book 2, Tyumen’, pp. 165–168.

Idelchik, I.E. (Ed.), 1992. Hydraulic Resistance. A Handbook. Mashinostroenie, Moscow, 616 pp. (in Russian)

Received April 7, 2016